DEPDC1B is involved in the proliferation, metastasis, cell cycle arrest and apoptosis of colon cancer cells by regulating NUP37

HUI XIONG[1*], YUN LI[1*] and MANHUA LIU[2]

[1]Department of General Surgery, The First Affiliated Hospital of Nanchang University, Nanchang, Jiangxi 330006; [2]Department of General Surgery, The First Affiliated Hospital of Nanchang University Jing'an County People's Hospital, Jing'an, Shanghai 330600, P.R. China

Received January 3, 2023; Accepted April 5, 2023

DOI: 10.3892/mmr.2023.13013

Abstract. It has been reported that DEP domain protein 1B (DEPDC1B) serves several roles in the occurrence and development of various types of cancer. Nevertheless, the effect of DEPDC1B on colorectal cancer (CRC), as well as its particular underlying molecular mechanism remain to be elucidated. In the present study, the mRNA and protein expression levels of DEPDC1B and nucleoporin 37 (NUP37) in CRC cell lines were assessed by reverse transcription-quantitative PCR and western blotting, respectively. Cell Counting Kit-8 and 5-Ethynyl-2'-deoxyuridine assays were carried out to determine cell proliferation. In addition, the migration and invasion abilities of cells were evaluated using wound healing and Transwell assays. The changes in cell apoptosis and cell cycle distribution were assessed by flow cytometry and western blotting. Bioinformatics analysis and co-immunoprecipitation assays were performed to predict and verify, respectively, the binding capacity of DEPDC1B on NUP37. The expression levels of Ki-67 were detected by immunohistochemical assay. Finally, the activation of phosphoinositide 3-kinase (PI3K)/protein kinase B (AKT) signaling was measured using western blotting. The results showed that DEPDC1B and NUP37 were upregulated in CRC cell lines. DEPDC1B and NUP37 silencing both inhibited the proliferation, migration and invasion capabilities of CRC cells and promoted cell apoptosis and cell cycle arrest. Furthermore, NUP37 overexpression reversed the inhibitory effects of DEPDC1B silencing on the behavior of CRC cells. Animal experiments demonstrated that DEPDC1B knockdown inhibited the growth of CRC *in vivo* by targeting NUP37. In addition, DEPDC1B knockdown inhibited the expression levels of the PI3K/AKT signaling-related proteins in CRC cells and tissues by also binding to NUP37. Overall, the current study suggested that DEPDC1B silencing could alleviate the progression of CRC via targeting NUP37.

Correspondence to: Professor Hui Xiong, Department of General Surgery, The First Affiliated Hospital of Nanchang University, 17 Yong Waizheng Street, Donghu, Nanchang, Jiangxi 330600, P.R. China
E-mail: xionghui0413@163.com

*Contributed equally

Key words: DEP domain protein 1B, nucleoporin 37, colon cancer, metastasis, apoptosis

Introduction

As a type of gastrointestinal cancer, colorectal cancer (CRC) can occur anywhere from the cecum to the rectum (1). Epidemiological studies have suggested that the incidence of colon cancer is higher in men compared with women (2). The incidence and mortality rates of colon cancer both increase progressively with age (3). The commonest treatment approaches for CRC include chemical and surgical therapy, and radiotherapy, along with targeted therapy (4). Surgical treatment is appropriate for patients with early tumors without invasion or metastasis. The majority of patients can be cured following surgical resection of the primary lesion, which is considered as the most effective treatment strategy for colon cancer (5). However, when the tumor reaches an intermediate and advanced stage, the effectiveness of surgical treatment is low, the risk of recurrence is greater and the quality of life of patients is also relatively poor (6). Therefore, the development of more effective treatment approaches and the identification of novel therapeutic targets for patients with CRC are of great significance.

Being located on chromosome 5 (5q12.1), DEP domain protein 1B (DEPDC1B) gene encodes a protein encompassing two conserved domains, namely DEP and RhoGAP (7). DEP, as a globular domain, can interact with G protein-coupled receptors (GPCRs) to regulate GPCR signaling. The RhoGAP domain is associated with Rho-GTPase signal transduction, which in turn is closely associated with cell proliferation, migration and invasion, cell cycle progression as well as cytoskeletal recombination (8). It has been reported that DEPDC1B is upregulated in several types of cancer, such as prostate cancer (PCa), soft tissue sarcoma, cervical cancer and malignant melanoma (9-12). A previous study indicated that DEPDC1B could promote the proliferation of oral cancer cells by regulating the Ras-related C3 botulinum toxin substrate 1 (Rac1)/extracellular signal-regulated protein kinase 1/2 signaling pathway (13). Another study revealed that

DEPDC1B, which could act as an oncogene in non-small cell lung cancer (NSCLC), was negatively associated with patient survival, while it could enhance the migration and invasion abilities of NSCLC cells by activating the Wnt/β-catenin pathway (14), but the role of DEPDC1B in CRC and its underlying mechanism has not yet reported. It has been reported that NUP37, as a component of the nuclear pore complex, serves a crucial role in the regulation of gene expression and heterochromatin function, as well as in the formation of the nuclear envelope (15). Huang *et al* (16) demonstrated that NUP37 deficiency could attenuate cell proliferation and induce G_1 phase cell cycle arrest and apoptosis in NSCLC cells. Furthermore, NUP37 could enhance the proliferation, migration and invasion abilities of gastric cancer cells via triggering the PI3K/AKT/mammalian target of rapamycin signaling pathway (17). However, the role of NUP37 in CRC and its association with DEPDC1B remain to be elucidated. Therefore, the current study aimed to explore the expression of DEPDC1B in CRC cells and uncover the effect of DEPDC1B on regulating CRC cell proliferation, metastasis, cell cycle and apoptosis.

Materials and methods

Bioinformatics analysis. The Coexpedia database (http://www.coexpedia.org/) was used to analyze the co-expression between DEPDC1B and nucleoporin 37 (NUP37). PPA_pred database (https://www.iitm.ac.in/bioinfo/PPA_Pred/prediction.html#) was used to predict the binding between DEPDC1B and NUP37.

Cell culture and treatment. The human CRC cell lines SW620, HCT8 and HCT116 were purchased from Procell Life Science & Technology Co., Ltd., while the human HIEC intestinal epithelial cell line was provided by Ningbo Mingzhou Biotechnology Co., Ltd. Cells were cultured in DMEM (Invitrogen; Thermo Fisher Scientific, Inc.) supplemented with 10% FBS and 1% penicillin/streptomycin solution at 37˚C in a humidified atmosphere with 5% CO_2.

Cell transfection. NUP37-specific pcDNA overexpression plasmid (Ov-NUP37) and the corresponding negative control (Ov-NC), the specific small interfering (si)RNA targeting DEPDC1B (si-DEPDC1B-1:5'-GAUUCUAAGUCAAAU GCAAAU-3'; si-DEPDC1B-2:5'-GAAGAGAUAUGGAAG UCUAUG-3'; 50 nM), the specific siRNA targeting NUP37 (si-NUP37-1: 5'-GAGUUGCUGUAAAGAUUAAAU-3'; si-NUP37-2: 5'-GUGUGUGUAUAUAUAUAUUU-3'; 50 nM) and the siRNA control (si-NC: 5'-UUCUCCGAA CGUGUCACGU-3'; 50 nM) were obtained from Shanghai GenePharma Co., Ltd. HCT8 cells were transfected with the above recombinants using Lipofectamine® 2000 (Invitrogen; Thermo Fisher Scientific, Inc.) for 48 h at 37˚C, according to the manufacturer's instructions. Subsequent experiments were performed 48 h post-transfection.

Cell Counting Kit-8 (CCK-8) assay. Following inoculation of untreated or transfected HCT8 cells into 96-well plates at a density of $5x10^4$ cells/ml, cells were cultured in DMEM with 10% FBS for 24, 48 and 72 h at 37˚C. Subsequently, cells were treated with 10 µl WST-8 (Beyotime Institute of Biotechnology) at 37˚C followed by incubation for an additional 2 h. The optical density value in each well was measured at a wavelength of 450 nm using a microplate reader.

5-Ethynyl-2'-deoxyuridine (EdU) assay. Following seeding into six-well plates ($4x10^5$ cells/well), HCT8 cells were cultured overnight at 37˚C. Subsequently, HCT8 cells were fixed with 4% polyformaldehyde for 15 min at room temperature and 0.5% Triton X-100 at room temperature for 15 min. Cells were then stained using the Cell-Light™ EdU Cell Proliferation Detection Assay (Invitrogen; Thermo Fisher Scientific, Inc.) at room temperature for 30 min followed by counterstaining with DAPI at room temperature for 10 min. Finally, five areas were randomly selected at x200 magnification under a fluorescent microscope (Nikon Corporation).

Wound healing assay. Following inoculation into a six-well plate, the transfected cells were cultured at 37˚C until they reached 80-90% confluency. Subsequently, a wound was created on the cell monolayer using a 20-µl pipette tip and cells were then cultured at 37˚C in serum-free medium. Following incubation for 24 h, the area occupied by the migrated cells in the wound was determined. The migration rate was calculated using the following formula: (Wound width at 0 h-wound width at 24 h)/wound width at 0 h x100%. Cells were analyzed at five randomly selected fields under a light microscope (magnification, x100).

Transwell assay. Initially, the Transwell chambers (Corning, Inc.) were pre-treated with 0.1 ml Matrigel (Becton-Dickinson) at 37˚C for 30 min. The collected cells (density, $2x10^5$ cells/ml) were cultured in DMEM supplemented with 1% FBS at 37˚C for 48 h. Cell suspensions were seeded into the top chamber, while the lower chamber was supplemented with medium containing 10% FBS at 37˚C for 48 h. Following incubation, a cotton swab was employed to remove cells on the upper surface of the Transwell membrane. Subsequently, invaded cells on the lower surface were fixed with 100% methanol for 10 min at room temperature, followed by staining with 0.1% crystal violet for 10 min at room temperature. Finally, the invaded cells were counted at five randomly selected fields under a light microscope (magnification, x100).

Co-immunoprecipitation (Co-IP) assay. Total proteins were extracted from cells ($4x10^7$) using an IP lysis buffer (20 mM Tris-HCl, 150 mM NaCl, 1% Triton X-100, pH 7.5). The supernatant was centrifuged at 14,000 x g at 4˚C for 10 min to obtain whole-cell extracts. A part of the cell lysate was isolated as input to correct for non-specific binding and 250 µl cell lysates were then cultivated with rabbit-IgG, followed by incubation with DEPDC1B (dilution, 1:100; cat no. 8283; ProSci, Inc.) or NUP37 antibody (dilution, 1:100; cat no. PAB088Hu01; Wuhan USCN Business Co., Ltd.) with Protein A/G PLUS-Agarose beads (MilliporeSigma) at 4˚C overnight. Subsequently, the precipitate was washed in lysis buffer and then centrifuged (700 x g at 4˚C for 5 min). After discarding the supernatant, 25 µl 2C loading buffer was added, and then samples were heated in boiling water for 7 min to elute proteins, followed by western blotting as mentioned below.

Flow cytometry. The FITC Annexin V/PI Apoptosis Detection kit I (Guangzhou RiboBio Co., Ltd.) was used to assess cell apoptosis. The PBS-rinsed HCT8 cells were re-suspended in binding buffer and were then supplemented with 5 μl Annexin V-FITC and 10 μl propidium iodide (PI; 10 mg/ml) and incubated for 15 min in the dark at room temperature. Cell apoptosis was analyzed using FlowJo software (FlowJo LLC). Cell apoptosis rate (the percentage of early + late apoptotic cells) was obtained from three different replications. Furthermore, cell cycle was also assessed by flow cytometry. Briefly, cells that were harvested using trypsinization, were fixed with 70% ethanol at 4˚C overnight, followed by staining with a solution containing 50 μg/ml PI and 100 μg/ml RNase I at room temperature for 1 h in PBS. Cell cycle was then analyzed at the Flow Cytometry Core Facility of University of Colorado Denver (UCD) with a FACScan flow cytometer (BD Biosciences).

RNA extraction and reverse transcription-quantitative (RT-q) PCR. Total RNA isolated from $1x10^4$ HCT8 cells utilizing TRIzol® reagent (Thermo Fisher Scientific, Inc.) according to the manufacturer's protocols was reverse transcribed into cDNA according to the manufacturer's protocols using the PrimeScript RT Master Mix kit (Perfect Real Time; Takara Bio, Inc.), according to the manufacturer's protocol. cDNA was amplified by qPCR using the SYBR Premix Ex Taq™ II kit (Takara Bio Inc.) according to the manufacturer's instructions. The thermocycling conditions were as follows: Initial denaturation at 95˚C for 10 min, followed by 40 cycles of 95˚C for 10 sec and 58˚C for 60 sec. The following primer pairs were used for qPCR: DEPDC1B forward, 5'-AGACCGTGG AGCTTTTTCGTG-3' and reverse, 5'-TTCAGGGCCGAA GTTTTGACT-3'; NUP37 forward, 5'-AAGAAGCAGACG TTGAAGGCA-3' and reverse, 5'-CTCTGGGCTCCAAGC TATGC-3'; and GAPDH forward, 5'-AATGGGCAGCCG TTAGGAAA-3' and reverse, 5'-GCGCCCAATACGACC AAATC-3'. The relative mRNA levels were determined using the $2^{-\Delta\Delta Cq}$ method (18). GAPDH mRNA level was used for normalization. RT-qPCR was performed in triplicate.

Xenograft experiments. All animal experiments were approved by The First Affiliated Hospital of Nanchang University (approval no. SD-2021-011) and strictly followed the Guidelines for the Care and Use of Laboratory Animals by the National Institute of Health (19). A total of 15 male BALB/c nude mice (Beijing Vital River Laboratory Animal Technology Co, Ltd.) were housed in a temperature-controlled room (22±1˚C) at 40-70% humidity with a 12-h light/dark cycle. The animals had free access to standard food pellets and water. All nude mice (aged, 4-5 weeks; weight, 18-20 g) were randomly divided into three groups (n=5/group). A total of $5x10^6$ cells transfected with si-DEPDC1B with or without Ov-NUP37, were subcutaneously injected into the right flank of each nude mouse. Tumor volume and body weight were measured every three days. Tumor volume was calculated using the following formula: Volume=(length x $width^2$)/2. The allowed maximum tumor diameter and volume were 1.5 cm and 2,000 mm^3, respectively. Any difficulties in eating and water intake, any symptoms of discomfort (self-harm, abnormal posture, respiratory distress, crying), the long-term appearance of abnormalities with no signs of recovery (diarrhea, bleeding, faeces on genital area), if the animal's distress was judged to be intolerable, such as heavy weight loss (≥20% within a few days) or the transplanted cancer cells grew to a size of ≥1.5 cm, were used as the humanitarian endpoints of the present study and the experiment was immediately terminated and the animal was sacrificed. After three weeks, mice were sacrificed by CO_2 (50% vol/min) asphyxiation followed by cervical dislocation. The tumor tissues were then weighed and subjected to immunohistochemical and western blot analyses.

Immunohistochemistry assay. Cancer tissues from mice were fixed with 4% paraformaldehyde for 24 h at room temperature, embedded in paraffin and cut into 5-μm sections. The sections were then re-hydrated and deparaffinized by immersion in xylene (100% x2) followed by immersion in a graded alcohol series (100% ethanol for 1 min twice; 95% ethanol for 1 min and 70% ethanol for 1 min twice). For antigen retrieval, the tissues were microwaved in citrate-buffered solution (pH 6.0) for 3 min. Following blocking with 10% goat serum for 30 min at room temperature, the sections were first probed with Ki-67 antibody (dilution, 1:300; cat no. ab15580; Abcam) at 4˚C overnight and then with HRP-labelled goat anti-rabbit secondary antibody (cat. no. ab6721; dilution, 1:1,000; Abcam) for 30 min at room temperature. Finally, the sections were first stained with DAB and then with hematoxylin for 3 min at room temperature. Images of the tissue sections in five randomly selected fields were captured under a light microscope (magnification, x100).

Western blotting. Total proteins were extracted from tissues and cells utilizing a RIPA buffer (Auragene Bioscience Co.) and were then quantified using a BCA Protein Assay kit (Beijing Dingguo Changsheng Biotechnology Co., Ltd.), according to the standard protocol. Following separation by 10% SDS-PAGE (Bio-Rad Laboratories, Inc.), the proteins (50 μg) were transferred onto PVDF membranes (MilliporeSigma). The membranes, which were first blocked in 5% non-fat milk for 1 h at 37˚C in 0.1% tris-buffered saline with 0.1% Tween-20 (TBST), were incubated with specific antibodies targeting DEPDC1B (1:1,000; cat. no. LS-C674693; LifeSpan Biosciences), MMP-2 (1:1,000; cat. no. ab92536; Abcam), MMP-9 (1:1,000; cat. no. ab76003; Abcam), Bcl-2 (1:1,000; cat. no. ab692; Abcam), Bax (1:1,000; cat. no. ab32503; Abcam), Cyclin D1 (1:1,000; cat. no. ab16663; Abcam), cyclin B1 (1:1,000; cat. no. ab32053; Abcam), NUP37 (1:1,000; cat. no. LS-C135188; LifeSpan Biosciences), phosphorylated (p-)PI3K antibody (1:1,000; cat. no. ab182651; Abcam), PI3K antibody (1:1,000; cat. no. ab86714; Abcam), p-Akt antibody (1:1,000; cat. no. ab38449; Abcam), Akt antibody (1:500, ab8805; Abcam) and GAPDH (1:2,500, ab9485; Abcam) at 4˚C overnight. Subsequently, the PBST-rinsed membranes were probed with the HRP-conjugated goat anti-rabbit or mouse secondary antibodies (cat. nos. sc-2004 or sc-2005; 1:5,000; Santa Cruz Biotechnology, Inc.) for 1 h at room temperature. Finally, the protein bands were visualized utilizing an ECL detection system (Beyotime Institute of Biotechnology), according to the manufacturer's protocol. Finally, the protein bands were quantified by means of densitometry (QuantityOne 4.5.0 software; Bio-Rad Laboratories, Inc.).

Statistical analysis. All data are expressed as the mean ± SD. The results were analyzed using SPSS software (version 18.0; SPSS, Inc.). Differences among multiple groups were analyzed

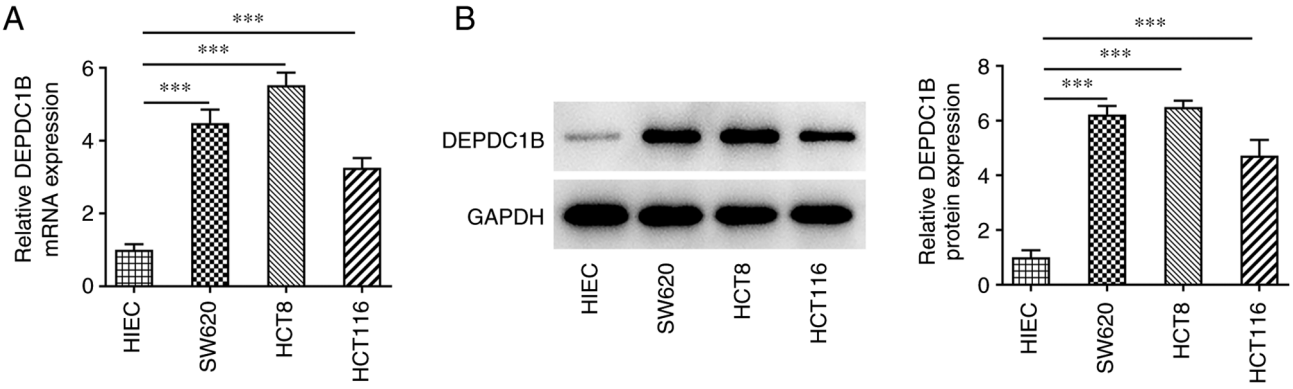

Figure 1. DEPDC1B expression was upregulated in CRC cells. The (A) mRNA and (B) protein levels of DEPDC1B were detected in several CRC cell lines by reverse transcription-quantitative PCR and western blotting. Data are expressed as mean ± SD. ***P<0.001. DEPDC1B, DEP domain protein 1B; CRC, colorectal cancer.

using one-way ANOVA with a post hoc Bonferroni multiple comparison test. P<0.05 was considered to indicate a statistically significant difference.

Results

DEPDC1B is upregulated in CRC cells. To investigate the role of DEPDC1B in CRC progression, the expression levels of DEPDC1B were detected in CRC cells. As shown in Fig. 1A and B, the mRNA and protein expression levels of DEPDC1B were notably increased in CRC cells compared with those in HIEC cells. Since HCT8 cells showed the highest DEPDC1B expression levels, these cells were used for the following experiments.

DEPDC1B silencing inhibits the proliferation, invasion and migration of CRC cells. To determine the biological role of DEPDC1B in CRC cells, a specific siRNA clone targeting DEPDC1B was transfected into HCT8 cells. The results demonstrated that the mRNA and protein expressions levels of DEPDC1B were conspicuously reduced following cell transfection with si-DEPDC1B (Fig. 2A and B). The si-DEPDC1B-1 clone exhibited the most potent silencing ability. Therefore, si-DEPDC1B-1 was chosen for the subsequent assays. Furthermore, CCK-8 assays showed that DEPDC1B silencing markedly suppressed cell viability (Fig. 2C). In addition, EdU assays demonstrated that the colony formation ability of DEPDC1B-depleted CRC cells was decreased compared with cells transfected with si-NC (Fig. 2D). Additionally, DEPDC1B knockdown attenuated the migration ability of HCT8 cells compared with the control group (Fig. 2E and F). Transwell assays also indicated that the invasion ability of HCT8 cells was restrained by DEPDC1B knockdown (Fig. 2G and H). Finally, western blotting showed that DEPDC1B silencing specifically decreased the protein expression levels of migration and invasion-related proteins MMP-2 and MMP-9 (Fig. 2I).

DEPDC1B silencing promotes CRC cell apoptosis and cell cycle arrest. Subsequently, the effect of DEPDC1B silencing on CRC cell apoptosis and cell cycle arrest was explored. As shown in Fig. 3A and B, the apoptosis rate of HCT8 cells transfected with si-DEPDC1B was notably elevated. In addition, the percentage of cells in the G_0/G_1 phase of the cell cycle was markedly increased, while that in the S phase was diminished in DEPDC1B-depleted cells, indicating the cell cycle was arrested after DEPDC1B silencing (Fig. 3C,D). Additionally, DEPDC1B knockdown in HCT8 cells upregulated Bax and downregulated Bcl-2, cyclin D1 and cyclin B1 (Fig. 3E).

DEPDC1B directly binds to NUP37. As shown in Fig. 4A and B, the mRNA and protein expression levels of NUP37 were significantly increased in CRC cells compared with the control group. The protein expression levels of NUP37 were notably reduced following DEPDC1B knockdown (Fig. 4C). Bioinformatics analysis using the Coexpedia database predicted that DEPDC1B was co-expressed with NUP37 and the score was 2.927 (Fig. 4D). Additionally, the Co-IP assay results verified the interaction between DEPDC1B and NUP37 (Fig. 4E).

NUP37 knockdown restrains the proliferation, invasion and migration of CRC cells. To investigate the effect of NUP37 on DEPDC1B-mediated CRC progression, NUP37 was silenced in HCT8 cells. The results revealed that NUP37 knockdown downregulated NUP37 in HCT8 cells (Fig. 5A and B). Evidently, si-NUP37-1 had an improved transfection efficiency compared with si-NUP37-1. Therefore, si-NUP37-1 was selected for the subsequent experiments. Additionally, the CCK-8 assay results showed that NUP37 silencing significantly attenuated the proliferation capability of HCT8 cells (Fig. 5C). Furthermore, NUP37 depletion reduced the number of positive-stained cells compared with the control group (Fig. 5D). In addition, wound healing and Transwell assays demonstrated that the migration and invasion abilities of HCT8 cells were markedly attenuated following NUP37 knockdown (Fig. 5E-H). Finally, western blotting demonstrated that MMP-2 and MMP-9 were both downregulated in NUP37-depleted cells (Fig. 5I).

NUP37 silencing accelerates the apoptosis and cycle arrest of CRC cells. As shown in Fig. 6A and B, NUP37 silencing obviously enhanced cell apoptosis compared with NC cells. The results obtained from flow cytometric assays demonstrated that the percentage of cells in the G_0/G_1 phase of the cell cycle was markedly increased, while the percentage of cells in the S

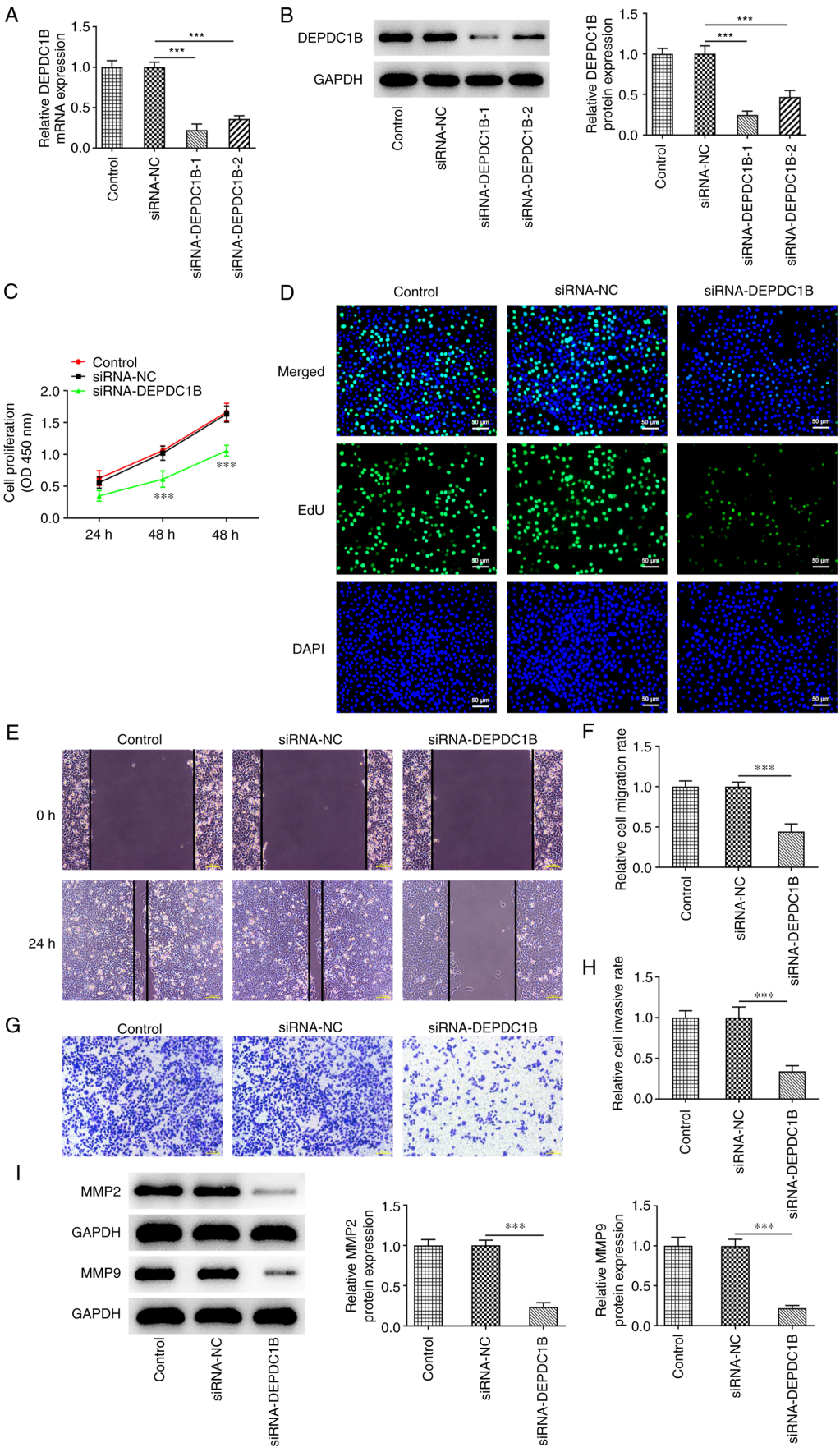

Figure 2. DEPDC1B silencing inhibits the proliferation, invasion and migration of CRC cells. The (A) mRNA and (B) protein levels of DEPDC1B were detected after the transfection with siRNA-DEPDC1B-1/2 by reverse transcription-quantitative PCR and western blotting. Cell proliferation was evaluated by (C) CCK-8 assay and (D) EdU assay. Original magnification, x200. (E and F) Cell migration was evaluated by wound healing assay. Original magnification, x100. (G and H) Cell invasion was evaluated by Transwell assay. Original magnification, x100. (I) Levels of MMP2 and MMP9 were measured by western blotting. Data are expressed as mean ± SD. ***P<0.001. DEPDC1B, DEP domain protein 1B; CRC, colorectal cancer; si, small interfering; NC, negative control.

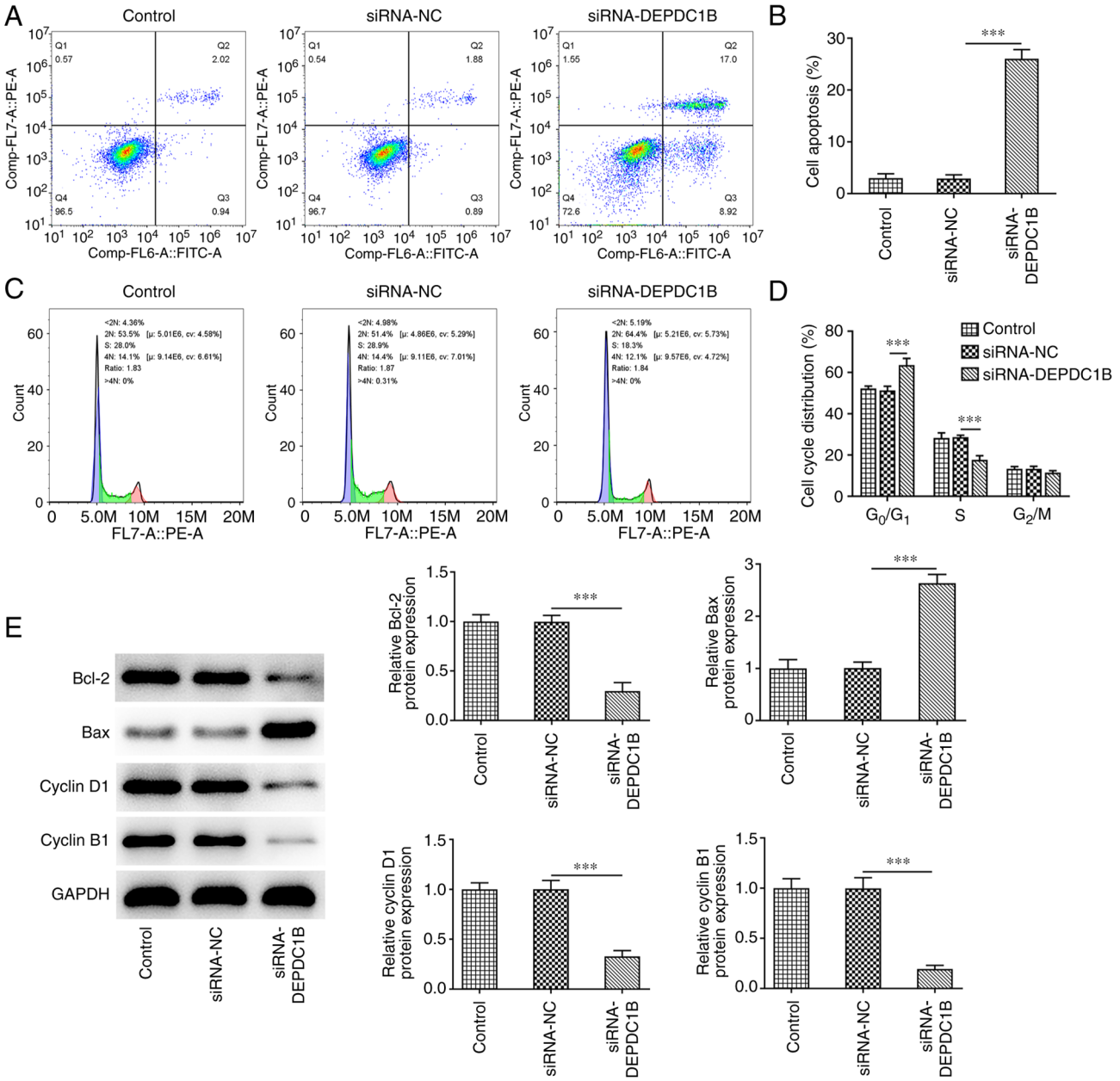

Figure 3. DEPDC1B silencing promotes apoptosis and cycle arrest of CRC cells. (A and B) Cell apoptosis was detected by flow cytometry. (C and D) Cell cycle was measured by flow cytometry analysis. (E) Western blotting was used to assess apoptotic-related and cell cycle-related protein levels. Data are expressed as mean ± SD. ***P<0.001. DEPDC1B, DEP domain protein 1B; CRC, colorectal cancer; si, small interfering; NC, negative control.

phase was reduced in NUP37-depleted cells (Fig. 6C and D). Finally, NUP37 deficiency decreased the levels of Bcl-2, cyclin D1 and cyclin B1, and increased those of Bax in HCT8 cells (Fig. 6E).

Overexpression of NUP37 reverses the effects of DEPDC1B knockdown on HCT8 cell proliferation, metastasis, apoptosis and cycle arrest. To further explore the biological function of NUP37 in HCT8 cells, NUP37 was overexpressed. The transfection efficiency is presented in Fig. 7A and B. As shown in Fig. 7C, NUP37 overexpression markedly strengthened the proliferation of DEPDC1B-depleted HCT8 cells. Additionally, NUP37 overexpression greatly increased the number of positive-stained cells (Fig. 7D). Wound healing and Transwell assays revealed that the cell migration and invasion rates were increased in NUP37-overexpressing cells (Fig. 7E-H). In addition, the western blotting results demonstrated that the protein levels of MMP2 and MMP9, the two protein that were associated with cell migration and invasion capacity, were enhanced in cells co-transfected with si-DEPDC1B and Ov-NUP37 (Fig. 7I). Additionally, the apoptosis rate of cells co-transfected with si-DEPDC1B and Ov-NUP37 was obviously decreased compared with cells transfected with si-DEPDC1B only (Fig. 8A and B). Furthermore, NUP37 overexpression reduced the number of cells in the G_0/G_1 phase of the cell cycle and increased those in the S phase in si-DEPDC1B-transfected cells (Fig. 8C and D). Finally, the levels of Bcl-2 and Bax were detected to assess the apoptotic levels, and the levels of cyclin D1 and cyclinB1 were detected to measure the cell cycle. The results showed that the protein expression levels of Bcl-2,

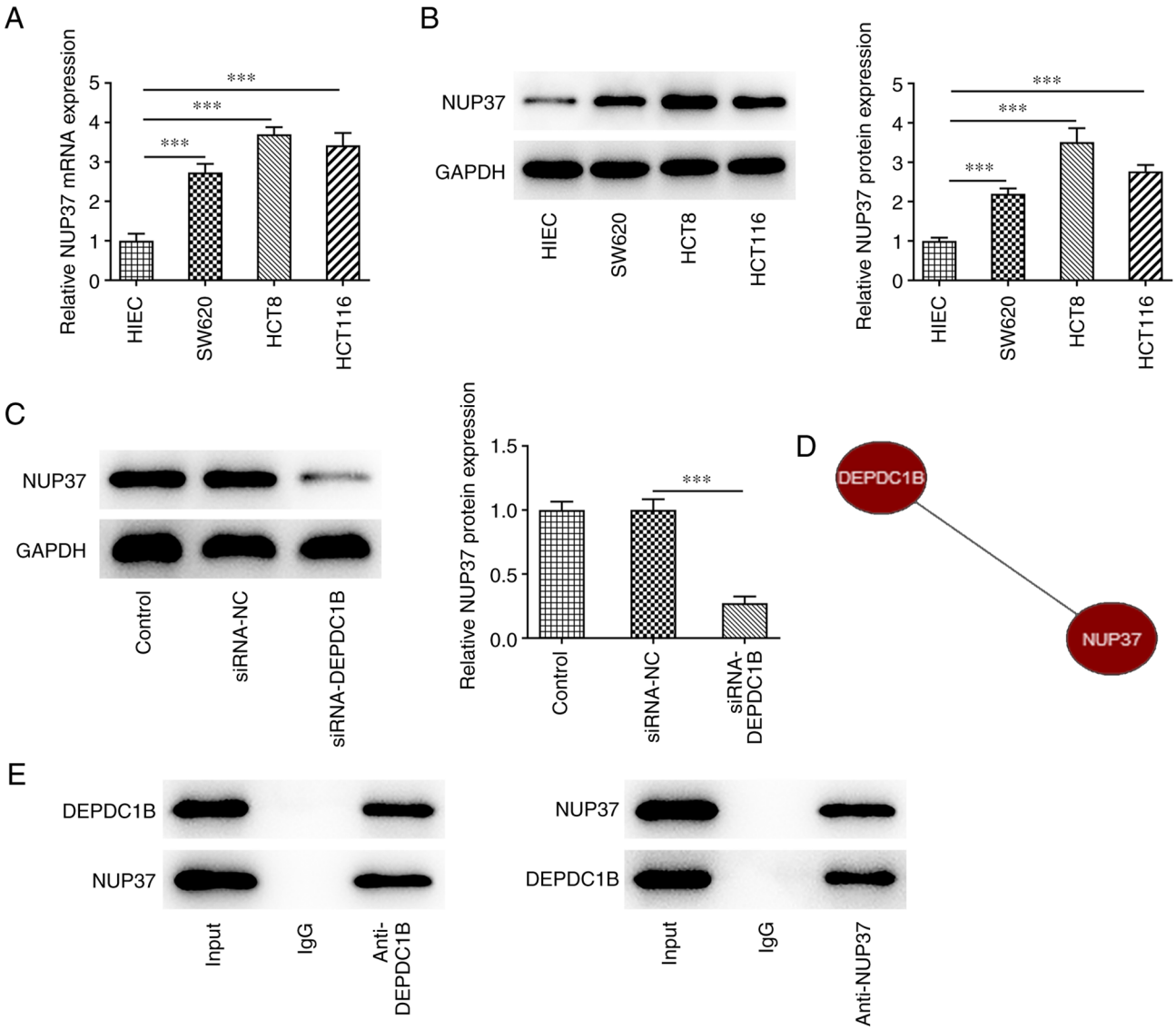

Figure 4. DEPDC1B binds to NUP37 directly. The (A) mRNA and (B) protein levels of NUP37 were detected in CRC cell lines by reverse transcription-quantitative PCR and western blotting. (C) Protein level of NUP37 in cells after the transfection with siRNA-DEPDC1B was detected by western blotting. (D) The Coexpedia database analyzed that DEPDC1B was co-expressed with NUP37. (E) Co-immunoprecipitation assay verified the combination of DEPDC1B and NUP37. Data are expressed as mean ± SD. ***P<0.001. DEPDC1B, DEP domain protein 1B; NUP37, nucleoporin 37; CRC, colorectal cancer; si, small interfering; NC, negative control.

cyclin D1 and cyclinB1 were increased and the level of Bax were reduced in NUP37 overexpressing cells (Fig. 8E).

DEPDC1B silencing inhibits the growth of CRC and the PI3K/AKT pathway in vivo via regulating NUP37. To further investigate the biological role of the DEPDC1B/NUP37 axis in CRC *in vivo*, HCT8 cells transfected with si-DEPDC1B or Ov-NUP37 were separately subcutaneously injected into the flanks of nude mice. As shown in Fig. 9A-C, DEPDC1B knockdown notably decreased tumor weight and volume compared with the control group. However, NUP37 overexpression reversed the effect of DEPDC1B silencing on tumor weight and volume. In addition, immunohistochemistry assays showed that the expression levels of Ki-67 were reduced in the tumor tissues of nude mice treated with si-DEPDC1B. However, NUP37 overexpression upregulated Ki-67 (Fig. 9D). To assess the extent of activation of the Akt-PI3K signaling pathway, the protein levels of p-PI3K, PI3k, p-AKT and AKT were detected. The western blotting results revealed that si-DEPDC1B reduced the phosphorylation of PI3K and AKT, while NUP37 overexpression reversed the effect of DEPDC1B knockdown on the expression levels of p-PI3K and p-AKT in HCT8 cells (Fig. 10A) and murine tissues (Fig. 10B).

Discussion

CRC is associated with 700,000 deaths every year, exceeded only by lung, liver and stomach cancers (20). Surgical resection is the mainstay of treatment, while systemic chemotherapy and local pelvic radiotherapy are critical adjuvant treatment modalities (21). However, the prognosis of CRC is far from satisfactory, particularly for patients suffering from metastatic lesions (22). Targeted therapy is a novel effective treatment approach, which can successfully prolong the overall survival

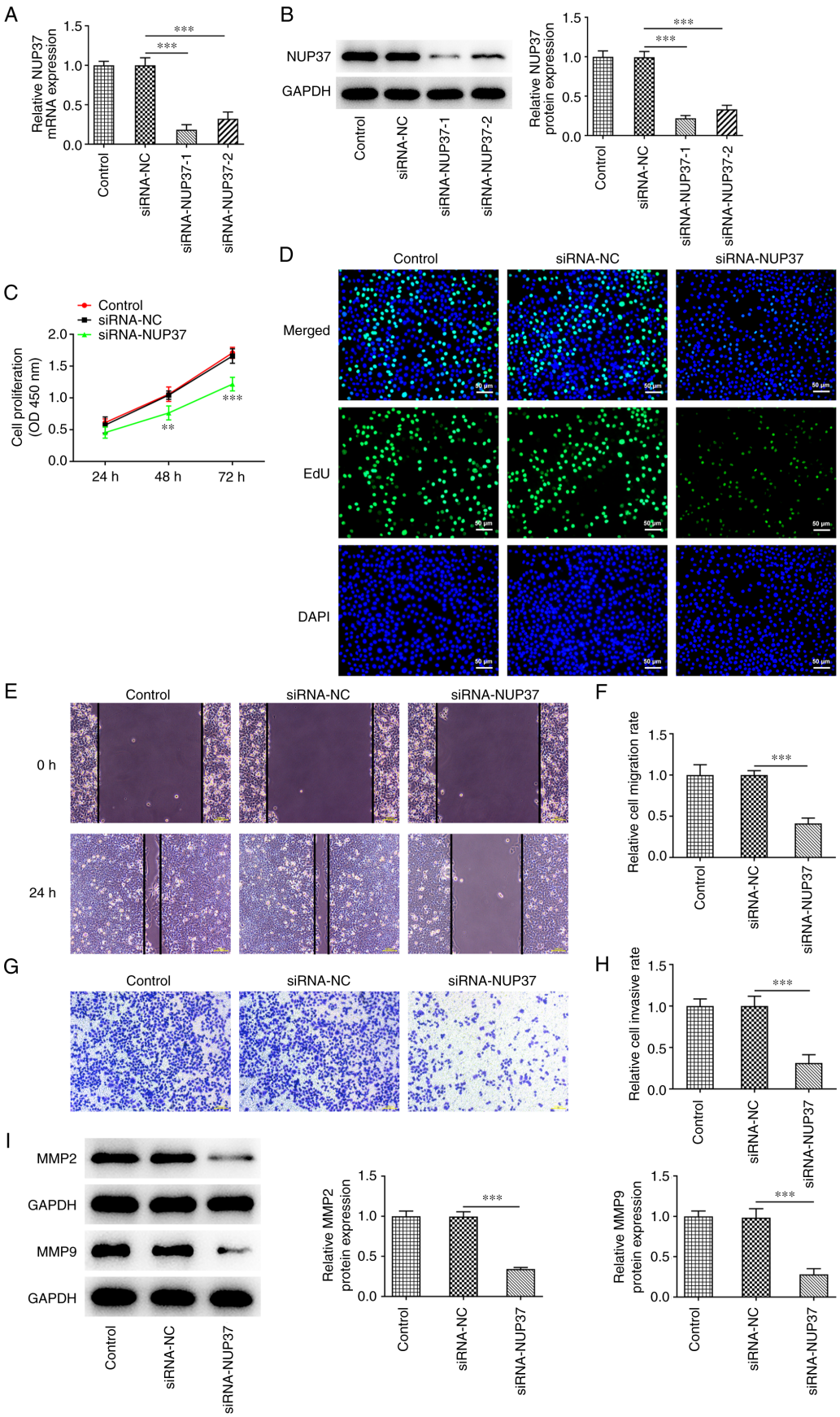

Figure 5. NUP37 knockdown restrains the proliferation, invasion and migration of CRC cells. The (A) mRNA and (B) protein levels of NUP37 were detected after transfection with siRNA-NUP37-1/2 by reverse transcription-quantitative PCR and western blotting. Cell proliferation was evaluated by (C) CCK-8 and (D) EdU assays. Original magnification, x200. (E and F) Cell migration was evaluated by wound healing assay. Original magnification, x100. (G and H) Cell invasion was evaluated by Transwell assay. Original magnification, x100. (I) Levels of MMP2 and MMP9 were measured by western blotting. Data are expressed as mean ± SD. **P<0.01, ***P<0.001. NUP37, nucleoporin 37; CRC, colorectal cancer; si, small interfering; EdU, 5-Ethynyl-2'-deoxyuridine; NC, negative control.

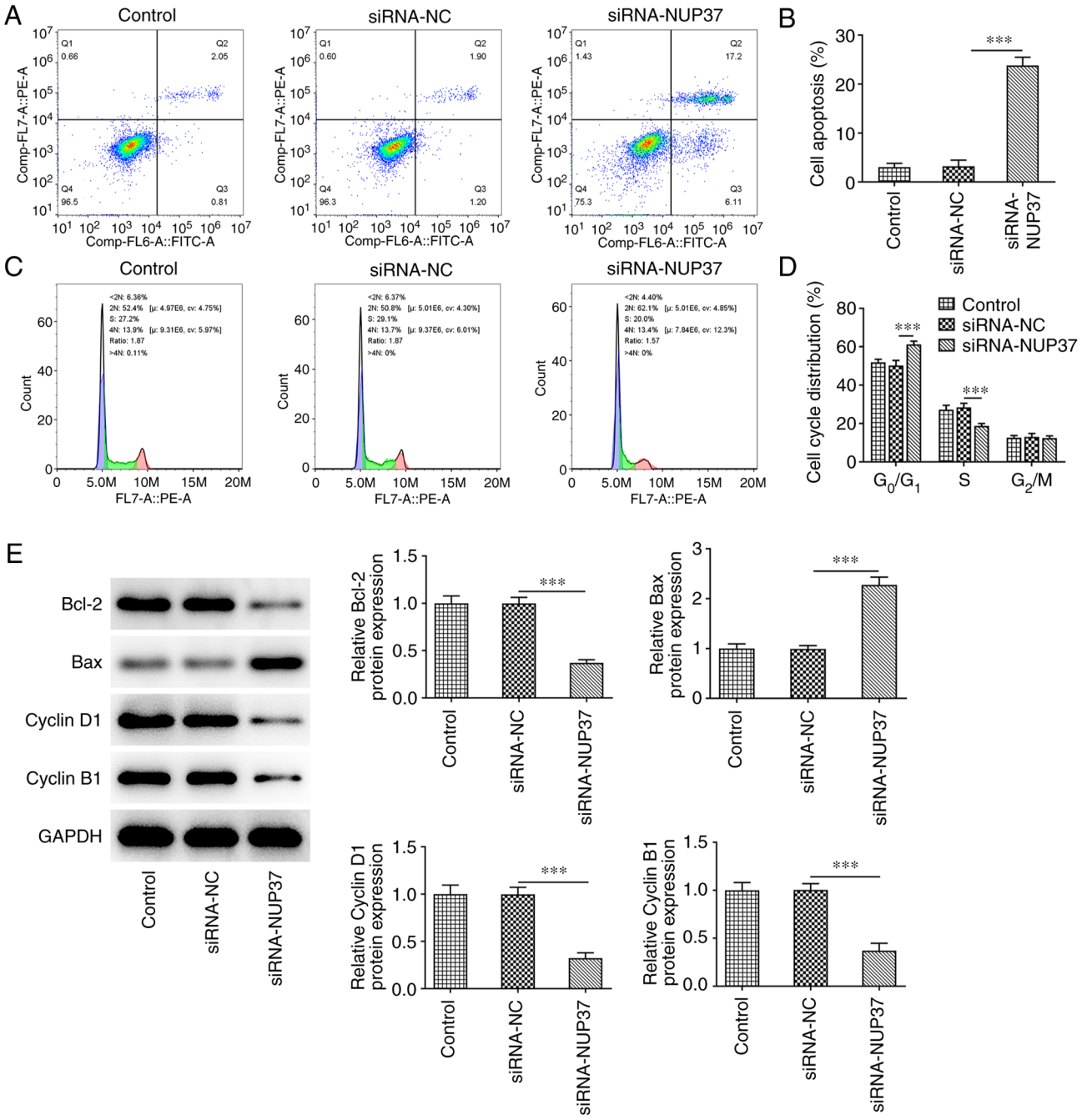

Figure 6. NUP37 silencing accelerates the apoptosis and cycle arrest of CRC cells. (A and B) Cell apoptosis was detected by flow cytometry. (C and D) Cell cycle was measured by flow cytometry analysis. (E) Western blotting was used to assess apoptosis- and cell cycle-related proteins. Data are expressed as mean ± SD. ***P<0.001. NUP37, nucleoporin 37; CRC, colorectal cancer; si, small interfering; NC, negative control.

of patients with CRC (23). The current study aimed to evaluate the therapeutic potential of DEPDC1B in CRC cell migration, apoptosis and cycle arrest and to uncover its underlying molecular mechanisms.

DEPDC1B is a recently identified gene located on human chromosome 5q12.1. It has been reported that DEPDC1B is involved in cell proliferation, apoptosis and cell cycle distribution (24). A previous study also demonstrated that DEPDC1B could critically regulate the progression of several types of cancer, such as hepatocellular and NSCLC (25). Li *et al* (26) showed that DEPDC1B is significantly upregulated in patients with PCa and is positively associated with a high Gleason score and poor prognosis. DEPDC1B increases the levels of Rac1-GTP to enhance the activation of the Rac1/p21activated kinase 1 signaling pathway, thus inducing epithelial-mesenchymal transition and promoting PCa metastasis and progression. Additionally, Lai *et al* (27) showed that DEPDC1B deficiency suppresses the proliferation and migration and promotes the apoptosis of bladder cancer cells both *in vitro* and *in vivo*. Nevertheless, the role of DEPDC1B in colon cancer remains to be elucidated. The results of the present study revealed that DEPDC1B was upregulated in CRC cell lines as well as in tissues derived from a CRC mouse

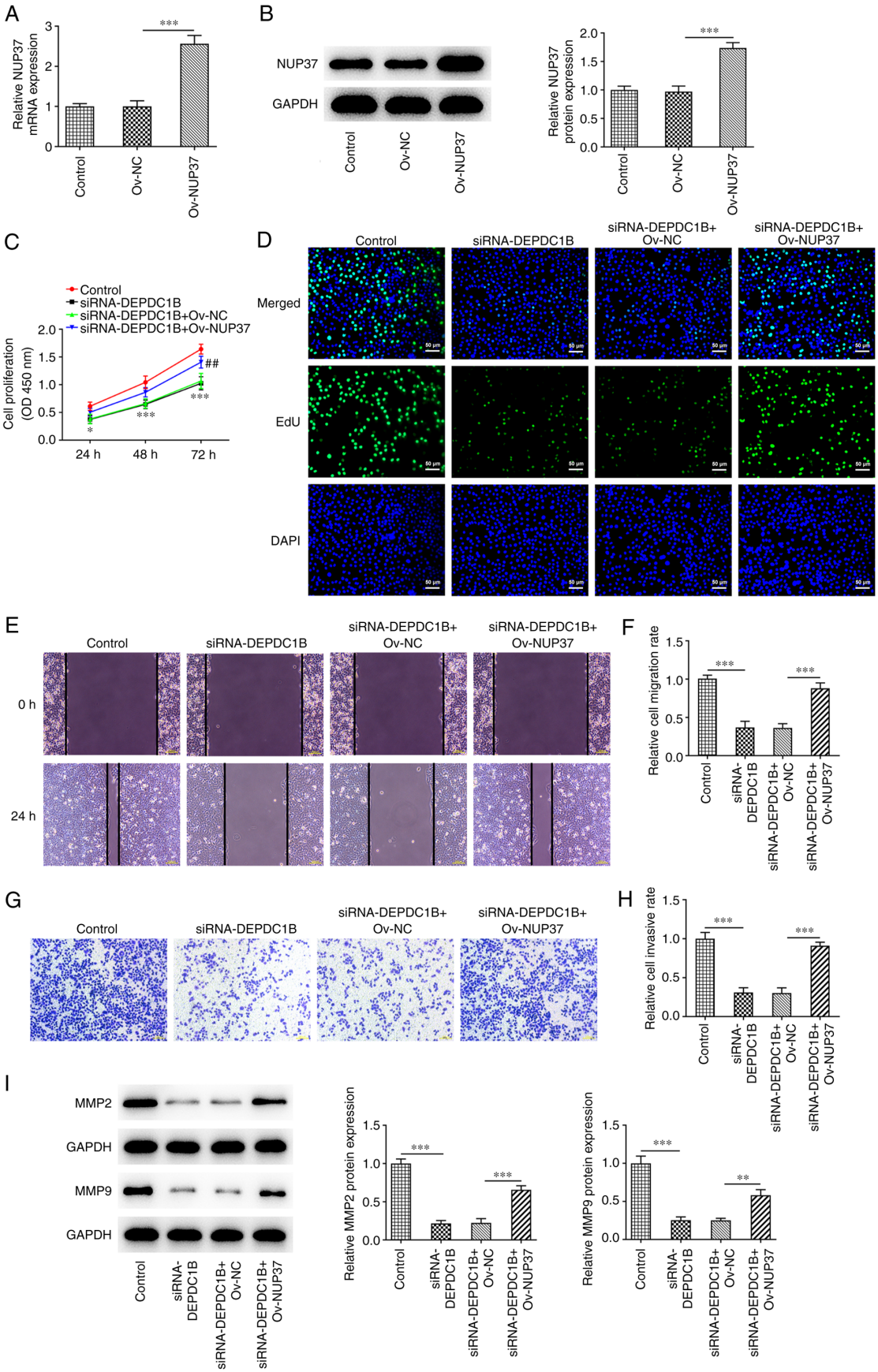

Figure 7. DEPDC1B knockdown inhibits the proliferation and metastasis of HCT8 cells through NUP37. The (A) mRNA and (B) protein levels of NUP37 were detected after the transfection with Ov-NUP37 by reverse transcription-quantitative PCR and western blotting. Cell proliferation was evaluated by (C) CCK-8 and (D) EdU assays. Original magnification, x200. (E and F) Cell migration was evaluated by wound healing assay. Original magnification, x100. (G and H) Cell invasion was evaluated by Transwell assay. Original magnification, x100. (I) Levels of MMP2 and MMP9 were measured by western blotting. Data are expressed as mean ± SD. *P<0.05, **P<0.01, ***P<0.001. DEPDC1B, DEP domain protein 1B; NUP37, nucleoporin 37; Ov, overexpression; si, small interfering; NC, negative control.

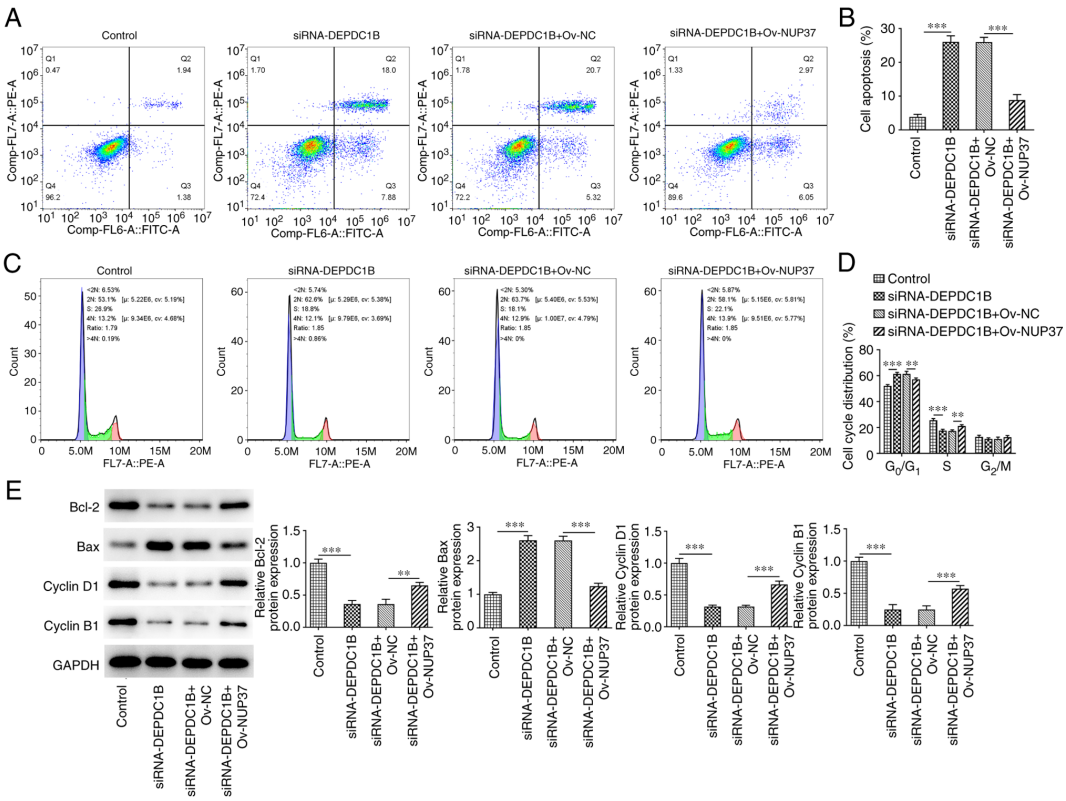

Figure 8. DEPDC1B knockdown facilitates the apoptosis and cycle arrest of HCT8 cells through NUP37. (A and B) Cell apoptosis was detected by flow cytometry. (C and D) Cell cycle was measured by flow cytometry analysis. (E) Western blotting was used to assess apoptosis- and cell cycle-related proteins. Data are expressed as mean ± SD. **P<0.01, ***P<0.001. DEPDC1B, DEP domain protein 1B; NUP37, nucleoporin 37; small interfering; NC, negative control; Ov, overexpression.

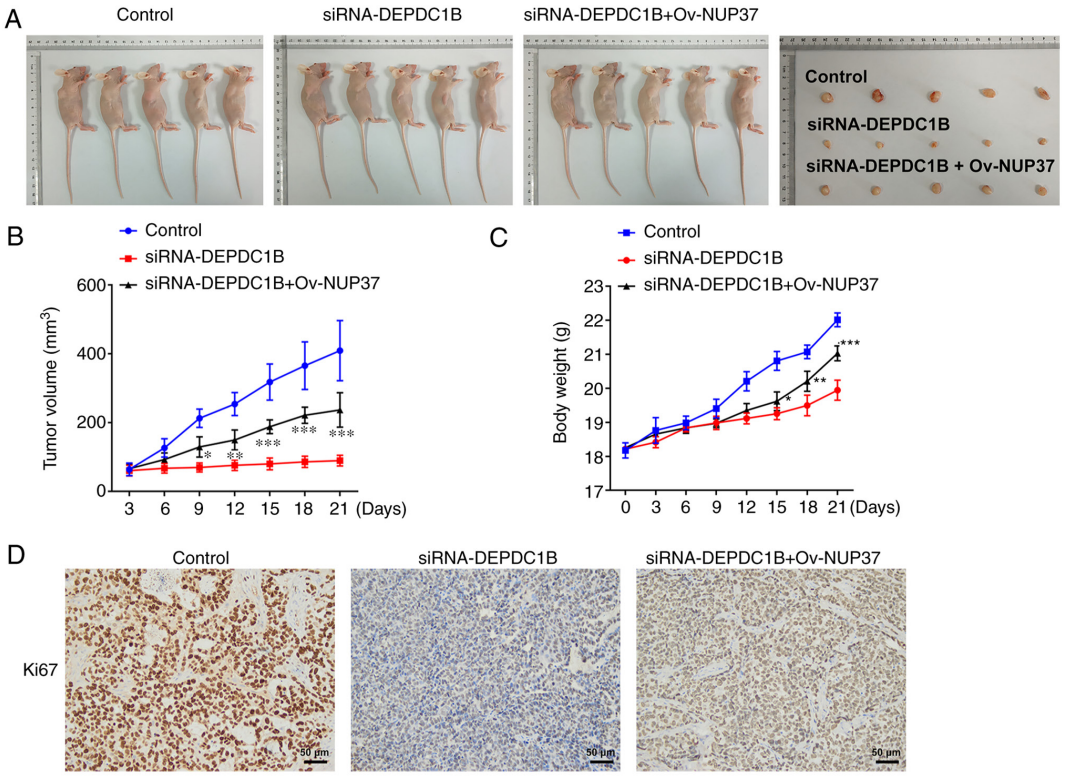

Figure 9. DEPDC1B silencing inhibits the growth of CRC *in vivo* through NUP37. (A) Mice were injected with HCT8 cells transfected with si-DEPDC1B and Ov-NUP37 and cancer tissues. (B) Weight of mice after the injection with si-DEPDC1B and Ov-NUP37. (C) Volume of tumor after the injection with si-DEPDC1B and Ov-NUP37. (D) Immunohistochemistry was used to assess the level of Ki-67 in cancer tissues of mice. Original magnification, x200. Data are expressed as mean ± SD. *P<0.05, **P<0.01, ***P<0.001. DEPDC1B, DEP domain protein 1B; CRC, colorectal cancer; NUP37, nucleoporin 37; si, small interfering; Ov, overexpression; NC, negative control.

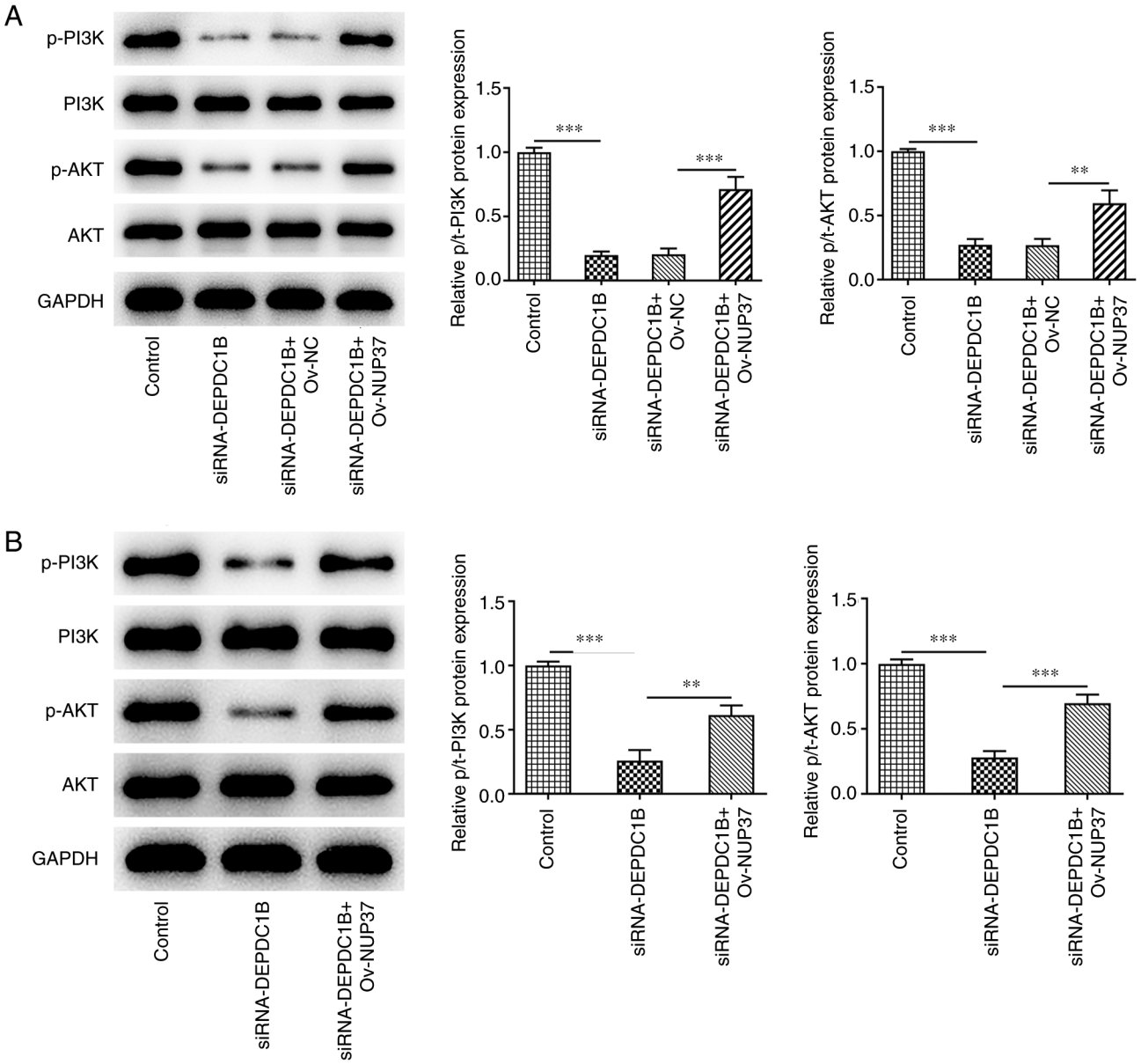

Figure 10. DEPDC1B silencing suppresses the PI3K/AKT pathway *in vivo* through NUP37. The protein expressions of PI3K/AKT pathway in (A) CRC cells and (B) mice tissues were detected by western bolt assay. Data are expressed as mean ± SD. **P<0.01, ***P<0.001. DEPDC1B, DEP domain protein 1B; NUP37, nucleoporin 37; CRC, colorectal cancer; p-, phosphorylated; si, small interfering; Ov, overexpression; NC, negative control.

model. In addition, DEPDC1B depletion attenuated the proliferation, migration and invasion abilities of CRC cells, while it promoted CRC cell apoptosis and cell cycle arrest by inhibiting Bcl-2 and promoting Bax level, as well as repressing cyclin D1 and cyclin B1.

To further reveal the mechanism underlying the effect of DEPDC1B on regulating colorectal adenocarcinoma, the Coexpedia database was used to predict the co-expression between DEPDC1B and NUP37. NUP37 was upregulated in CRC cell lines and its protein expression levels were significantly decreased following DEPDC1B knockdown. Co-IP assays also verified the interaction between DEPDC1B and NUP37. In addition, NUP37 knockdown attenuated the proliferation, migration and invasion capabilities of CRC cells, while it accelerated cell apoptosis and cell cycle arrest, which were then reversed by NUP37 overexpression.

Previous studies show that both DEPDC1B and NUP37 can promote the expression of PI3K/AKT signaling-related proteins (28,29). Therefore, the current study aimed to investigate whether DEPDC1B could be involved in the regulation of PI3K/AKT signaling via targeting NUP37. Functional experiments indicated that DEPDC1B deficiency could conspicuously inhibit the PI3K/AKT signaling pathway. However, NUP37 overexpression reversed the effects of DEPDC1B silencing on PI3K/AKT signaling both *in vitro* and *in vivo*.

There are several limitations to the present study. It did not explore the roles of DEPDC1B overexpression in HCT8 cells. In addition, CRC clinical specimens were not involved in this study. Moreover, the present study only performed assays in one cell line HCT8; using several cell lines may improve the results and will be considered in a further study.

In conclusion, the results of the present study suggested that DEPDC1B silencing could inhibit the proliferation, migration and invasion abilities and enhance the apoptosis and cell cycle arrest of CRC cells via NUP37. The above findings could provide a novel insight into prospective strategies for treating CRC.

Acknowledgements

Not applicable.

Funding

No funding was received.

Availability of data and materials

All data generated or analyzed during this study are included in this published article.

Authors' contributions

HX and YL designed the study, drafted and revised the manuscript. HX and ML analyzed the data and searched the literature. All authors performed the experiments and all authors read and approved the final manuscript. HX and YL confirm the authenticity of all the raw data.

Ethics approval and consent to participate

All of the experimental protocols were approved by The First Affiliated Hospital of Nanchang University (approval no. SD-2021-011) and strictly followed the Guidelines for the Care and Use of Laboratory Animals by National Institute of Health.

Patient consent for publication

Not applicable.

Competing interests

The authors declare that they have no competing interests.

References

1. Li J, Ma X, Chakravarti D, Shalapour S and DePinho RA: Genetic and biological hallmarks of colorectal cancer. Genes Dev 35: 787-820, 2021.
2. Baidoun F, Elshiwy K, Elkeraie Y, Merjaneh Z, Khoudari G, Sarmini MT, Gad M, Al-Husseini M and Saad A: Colorectal cancer epidemiology: Recent trends and impact on outcomes. Curr Drug Targets 22: 998-1009, 2021.
3. Dekker E, Tanis PJ, Vleugels JLA, Kasi PM and Wallace MB: Colorectal cancer. Lancet 394: 1467-1480, 2019.
4. Heinimann K: Hereditary colorectal cancer: Clinics, diagnostics and management. Ther Umsch 75: 601-606, 2018 (In German).
5. Zielińska A, Włodarczyk M, Makaro A, Sałaga M and Fichna J: Management of pain in colorectal cancer patients. Crit Rev Oncol Hematol 157: 103122, 2021.
6. Sinha R: Colorectal cancer. Clin Radiol 76: 870, 2021.
7. Wang L, Tang L, Xu R, Ma J, Tian K, Liu Y, Lu Y, Wu Z and Zhu X: DEPDC1B regulates the progression of human chordoma through UBE2T-mediated ubiquitination of BIRC5. Cell Death Dis 12: 753, 2021.
8. Figeac N, Pruller J, Hofer I, Fortier M, Ortuste Quiroga HP, Banerji CRS and Zammit PS: DEPDC1B is a key regulator of myoblast proliferation in mouse and man. Cell Prolif 53: e12717, 2020.
9. Bai S, Chen T, Du T, Chen X, Lai Y, Ma X, Wu W, Lin C, Liu L and Huang H: High levels of DEPDC1B predict shorter biochemical recurrence-free survival of patients with prostate cancer. Oncol Lett 14: 6801-6808, 2017.
10. Pollino S, Benassi MS, Pazzaglia L, Conti A, Bertani N, Righi A, Piccinni-Leopardi M, Picci P and Perris R: Prognostic role of XTP1/DEPDC1B and SDP35/DEPDC1A in high grade soft-tissue sarcomas. Histol Histopathol 33: 597-608, 2018.
11. Zhang F and Zhou Q: Knockdown of BRCC3 exerts an anti-tumor effect on cervical cancer *in vitro*. Mol Med Rep 18: 4886-4894, 2018.
12. Xu Y, Sun W, Zheng B, Liu X, Luo Z, Kong Y, Xu M and Chen Y: DEPDC1B knockdown inhibits the development of malignant melanoma through suppressing cell proliferation and inducing cell apoptosis. Exp Cell Res 379: 48-54, 2019.
13. Su YF, Liang CY, Huang CY, Peng CY, Chen CC, Lin MC, Lin RK, Lin WW, Chou MY, Liao PH and Yang JJ: A putative novel protein, DEPDC1B, is overexpressed in oral cancer patients, and enhanced anchorage-independent growth in oral cancer cells that is mediated by Rac1 and ERK. J Biomed Sci 21: 67, 2014.
14. Yang Y, Liu L, Cai J, Wu J, Guan H, Zhu X, Yuan J and Li M: DEPDC1B enhances migration and invasion of non-small cell lung cancer cells via activating Wnt/β-catenin signaling. Biochem Biophys Res Commun 450: 899-905, 2014.
15. Walther TC, Alves A, Pickersgill H, Loïodice I, Hetzer M, Galy V, Hülsmann BB, Köcher T, Wilm M, Allen T, *et al*: The conserved Nup107-160 complex is critical for nuclear pore complex assembly. Cell 113: 195-206, 2003.
16. Huang L, Wang T, Wang F, Hu X, Zhan G, Jin X, Zhang L and Li Y: NUP37 silencing induces inhibition of cell proliferation, G1 phase cell cycle arrest and apoptosis in non-small cell lung cancer cells. Pathol Res Pract 216: 152836, 2020.
17. Zhang J, Lv W, Liu Y, Fu W, Chen B, Ma Q, Gao X and Cui X: Nucleoporin 37 promotes the cell proliferation, migration, and invasion of gastric cancer through activating the PI3K/AKT/mTOR signaling pathway. In Vitro Cell Dev Biol Anim 57: 987-997, 2021.
18. Livak KJ and Schmittgen TD: Analysis of relative gene expression data using real-time quantitative PCR and the 2(-Delta Delta C(T)) method. Methods 25: 402-408, 2001.
19. National Research Council (US): Committee for the update of the guide for the care and use of laboratory animals: The national academies collection: Reports funded by national institutes of health. In: Guide for the care and use of laboratory animals. 8th edition. National Academies Press (US). National Academy of Sciences, Washington, DC, 2011.
20. Mármol I, Sánchez-de-Diego C, Pradilla Dieste A, Cerrada E and Rodriguez Yoldi MJ: Colorectal Carcinoma: A general overview and future perspectives in colorectal cancer. Int J Mol Sci 18, 2017.
21. Johdi NA and Sukor NF: Colorectal cancer immunotherapy: Options and strategies. Front Immunol 11: 1624, 2020.
22. Siegel RL, Miller KD and Jemal A: Cancer statistics, 2019. CA Cancer J Clin 69: 7-34, 2019.
23. Xie YH, Chen YX and Fang JY: Comprehensive review of targeted therapy for colorectal cancer. Signal Transduct Target Ther 5: 22, 2020.
24. Marchesi S, Montani F, Deflorian G, D'Antuono R, Cuomo A, Bologna S, Mazzoccoli C, Bonaldi T, Di Fiore PP and Nicassio F: DEPDC1B coordinates de-adhesion events and cell-cycle progression at mitosis. Dev Cell 31: 420-433, 2014.
25. Sun Y and Zhang Z: In silico identification of crucial genes and specific pathways in hepatocellular cancer. Genet Test Mol Biomarkers 24: 296-308, 2020.
26. Li Z, Wang Q, Peng S, Yao K, Chen J, Tao Y, Gao Z, Wang F, Li H, Cai W, *et al*: The metastatic promoter DEPDC1B induces epithelial-mesenchymal transition and promotes prostate cancer cell proliferation via Rac1-PAK1 signaling. Clin Transl Med 10: e191, 2020.
27. Lai CH, Xu K, Zhou J, Wang M, Zhang W, Liu X, Xiong J, Wang T, Wang Q, Wang H, *et al*: DEPDC1B is a tumor promotor in development of bladder cancer through targeting SHC1. Cell Death Dis 11: 986, 2020.
28. Liu X, Li T, Huang X, Wu W, Li J, Wei L, Qian Y, Xu H, Wang Q and Wang L: DEPDC1B promotes migration and invasion in pancreatic ductal adenocarcinoma by activating the Akt/GSK3β/Snail pathway. Oncol Lett 20: 146, 2020.
29. Yuan Y, Ping W, Zhang R, Hao Z and Zhang N: DEPDC1B collaborates with GABRD to regulate ESCC progression. Cancer Cell Int 22: 214, 2022.